A Novel Image Inpainting Technique Based on Isotropic Diffusion

Zainab A. Abdul Karim[1,*], Ahmed K. Al-Jaberi[2]

1. Department of Mathematics, College of Science, University of Basrah, Basrah, Iraq.

2. Department of Mathematics, College of Education for Pure Science, University of Basrah, Basrah, Iraq.

*Corresponding author: E-mail: zayanb.eali.sci@uobasrah.edu.iq

Doi:

ARTICLE INFO	**ABSTRACT**
Keywords Image inpainting. isotropic equation. PDE-based inpainting method. Image quality assessments. .	Using the isotropic diffusion model as a foundation, a novel method for image inpainting was suggested. To restore various missing areas of diverse natural images, a modified version of the original isotropic model is used. When employing the original isotropic model, the results of the suggested technique are compared to those obtained results. Regarding building texture in the missing area and restoring significant missing sections, the results of the suggested model performed better than the results of the obtained isotropic model. The performance of the suggested model in comparison to the original isotropic model is examined using a number of picture quality measures, including MSE, PSNR, and SSIM. In comparison to the widely used isotropic model, the improved model performs better and provides better measures of quality assessment for a greater number of natural photos.

1. **Introduction**

The goal of image inpainting is to repair the damaged area of the image and provide a high-quality semantic approximation of the original image [1]. Inpainting of damaged paintings was first used in art, where it was done by skilled painters. In contrast, inpainting in mathematics relates to the process of filling in damaged areas in an image by propagating information from surrounding areas [2]. In order to make the recognition process as simple and automatic as possible, improving the quality of damaged and noisy images is a vital challenge in image processing. As a result, image inpainting emerged as a significant study area with several potential applications in sectors as diverse as augmented reality, art, medical imaging, and computer-assisted restoration, as well as virtual restoration of digital artworks [3, 4]. Inpainting algorithms could be classified into three main approaches diffusion-based, exemplar-based [5], and machine learning-based ways [5]. Masnou and Morel initially suggested the diffusion-based approach, which produces results with strong discontinuities when level lines are used as the basis for the disocclusion. [6]. Diffusion partial differential equation (PDE) was used by Bertalmio et al. to resolve the inpainting process, in which boundary information propagates into the area to be painted in the direction of isophotes. [7]. Since PDE-based approaches are founded on and supported by the theory of PDEs and numerical analysis, they are theoretically sound and computationally efficient. As a result, a novel model for inpainting problem solving with an economical technique of solution was suggested by PDEs approaches. [8]. Nevertheless, there are two types of PDE approaches: linear (isotropic) and non-linear (anisotropic), with linear models being the most traditional and basic ones used to restore the missing region in the images. Although liner models have a noticeable smoothing effect on the missing region, they also damage other crucial aspects of the image, such as the edge, which appears blurry, especially when there is a significant missing area. As a result, several nonlinear models are proposed to solve this problem by slowing the diffusion at the edges [9]. Isotropic models are effective in removing noise, even if they fail to restore the borders of the images and provide an image that is similar to the original image. It is difficult and still not fully solved to develop an accurate assessment system that concurrently evaluates inpainted images [10]. As a result, visual analysis is used to evaluate the quality of inpainted images, while quantitative evaluation was established using statistical measures. The quality of the inpainted image produced by the original and updated isotropic models is estimated using Mean Squared Error (MSE), Structural Similarity (SSIM), and Peak Signal-to-Noise Ratio (PSNR) [8, 11]. When compared to the original isotropic model, the outcomes of the current work's isotropic model-based inpainting

have been improved. In the current study, a novel method for inpainting images based on an isoptrobic model has been proposed and put to the test in the current study. Additionally, the improved model's numerical solution was investigated.

2. Isotropic Diffusion Model

Diffusion-based inpainting is the first model was used to recover the damaged or missing part of the image by spreading information from the surrounding area of the missing region at the pixel point [12, 13]. However, the isotropic diffusion is the second order linear parabolic equation. Let $f \in L^2(\Omega)$ is an image and $D \subset \Omega$ is a missing information region from the original image; u is the inpainted image given by the solution of the below equation [14]:

$$\begin{cases} u_t = \Delta u, & t \geq 0 \\ \quad u(0, x, y) = 0. \end{cases} \qquad 1$$

In addition, u can be calculated from the solution of minimization functional for the squared total variation. Heat equation was introduced as minimization energy functional as [15]:

$$\min_{u \in L^2(\Omega)} \left\{ \iint |\nabla u|^2 \; dxdy \quad such \; that \quad u = f \; in \; \Omega \backslash D \right\} \qquad 2$$

Euler- Lagrange equation and gradient descent method are applied on the minimization functional 2, we get

$$u_t = \Delta u \qquad 3$$

The solution of equation 1 or 3 with the Dirichlet boundary condition is used to recover the missing regions in the image. The explicit finite difference method (EFEM) applied to find the solution of equation 1 or 3, which is imitative the solution of the heat equation on the spatial (image) domain. This equation is studied the spreading of temperatures (information) within a period in all directions based on the boundary condition [13]. However, the spread in all directions will cause failure to recover edge construction of the missing area and appear blurred under the isotropic model. The diffusion term comes from the idea of propagating local information with smoothness constraints by analogy with some physical phenomena like heat propagation in physical structures [6]. Isotropic diffusion acts as low-pass linear filtering suppressing high frequencies in the image thus, it works to minimize these variations in all directions that in turn led to appearing blurred close to edges and contours. More general formalisms using nonlinear PDEs are used for describing the physical and fluid dynamics phenomena to get better restoration of edges and more sharpness [9].

3. **Modify The Isotropic Diffusion Model**

The isotropic diffusion model is modified by adding more than one algebraic expression to reduce the blurry of the large missing area and enhance the edge of restoration. Modified isotropic model is proposed by adding the first derivative of the missing area of the image. The ability of the first derivative helps to build the edges and extend the isophote line, which improves of recovering missing areas. The modified isotropic equation writes as follows:

$$u_t = \Delta u + \alpha u_x + \beta u_y, \quad t \geq 0 \qquad\qquad 4$$

Where u_x and u_y are first derivatives of image, the α and β are coefficients. Furthermore, the value of α and β play an important effect on the values of quality measures. The numerical solutions of modified isotropic diffusion model give in next section.

3.1. Numerical Solution Of The Modified Isotropic Equation

The EFDM is used to find the numerical solution of the modified equation with Dirichlet boundary conditions. A dopt the notation

$$U = u(x,y,t) = u(i\Delta x, j\,\Delta y, n\Delta t) = u_{i,j}^n \qquad\qquad 5$$

The derivative formula becomes:

$$u_x(i\Delta x, j\,\Delta y, n\Delta t) = \frac{\partial u(i\Delta x, j\,\Delta y, n\Delta t)}{\partial x} = \frac{u_{i+1,j}^n - u_{i-1,j}^n}{2\Delta x} \qquad\qquad 6$$

$$u_y(i\Delta x, j\,\Delta y, n\Delta t) = \frac{\partial u(i\Delta x, j\,\Delta y, n\Delta t)}{\partial y} = \frac{u_{i,j+1}^n - u_{i,j-1}^n}{2\Delta y} \qquad\qquad 7$$

The modified isotropic equation formula is given by:

$$U_t = U_{xx} + U_{yy} + \alpha U_x + \beta U_y \qquad\qquad 8$$

The modified isotropic equation in eq.8 is rewritten using the EFDM:

$$u_{i,j}^{n+1} = \frac{\Delta t}{\Delta x^2}\left[u_{i+1,j}^n - 2u_{i,j}^n + u_{i-1,j}^n\right] + \frac{\Delta t}{\Delta y^2}\left[u_{i,j+1}^n - 2u_{i,j}^n + u_{i,j-1}^n\right] + u_{i,j}^n + \alpha\Delta t\left(\frac{u_{i+1,j}^n - u_{i-1,j}^n}{2\Delta x}\right) +$$

$$\beta\Delta t\left(\frac{u_{i,j+1}^n - u_{i,j-1}^n}{2\Delta y}\right) \qquad\qquad 9$$

Where $\Delta x = \Delta y = h = 1$. Let $\frac{\Delta t}{h^2} = r$, $\Delta t = 0.005$. Thus, the equation 9 will be:

$$u_{i,j}^{n+1} = ru_{i+1,j}^n - 4ru_{i,j}^n + ru_{i-1,j}^n + ru_{i,j+1}^n + ru_{i,j-1}^n + u_{i,j}^n + \frac{\alpha\Delta t}{2}\left(u_{i+1,j}^n - u_{i-1,j}^n\right) +$$

$$\frac{\beta\Delta t}{2}\left(u_{i,j+1}^n - u_{i,j-1}^n\right) \qquad\qquad 10$$

However, eq. 10 can be simplified to be equation 11:

$$u_{i,j}^{n+1} = (1 - 4r)u_{i,j}^n + (r + \frac{\alpha\Delta t}{2})u_{i+1.j}^n + (r - \frac{\alpha\Delta t}{2})u_{i-1,j}^n + (r + \frac{\beta\Delta t}{2})u_{i,j+1}^n + (r - \frac{\beta\Delta t}{2})u_{i,j-1}^n$$

$$11$$

The stability of the modified model is studied using different values of α and β and found that the model will be stable when: $0 \leq \alpha \leq 1,\ 0 \leq \beta \leq 1$, and $\alpha + \beta \leq 1$. Three cases of α and β values are selected to test the modified model depending on the texture direction. When the texture direction is horizontally extended, the values of α=0 and β=1 while α=1 and β=0 are selected for the vertically extended texture direction. However, for diagonal texture, the $\alpha, \beta \in (0,1);\ \alpha + \beta < 1$. Thus, the third case for diagonal texture was studied using $\alpha = \beta = 1/2$. Figure1 shows an image containing vertical twigs that are inpainted using three suggested values of $\alpha = \beta = 1/2$ in Figure1c, $\alpha = 1$ and $\beta = 0$ in Figure1d, and $\alpha = 0$, and $\beta = 1$ in Figure1e. When $\alpha = \beta = 1/2$ are selected, the twigs in the inpainted image appeared slant due to the two derivatives existing in the modified model and have the same effect on the direction of the derivative. However, when $\alpha = 1$ and $\beta = 0$, the restoration of twigs in the inpainted image was good because the texture was in the same direction with derivative diffusion (u_x) while when $\alpha = 0$ and $\beta = 1$, the restoration of twigs is failed due to the direction of texture was reversed the direction derivative diffusion (u_y).

Figure1: Effect of α and β values on image inpainting, (a) original image, (b) masked image, (c) inpainted image with α=β=1/2, (d) inpainted image with α=1, β=0, and (e) inpainted image with α=0, β=1

3.2 Stability of Modify Isotropic Model

Numerical stability problems related to some finite difference (FD)approximations of two dimensional modify isotropic model. The isotropic equation formula given by:

$$u_t = K(u_{xx} + u_{yy}) \qquad\qquad 12$$

modify isotropic model when k>0:

$$u_t = K(u_{xx} + u_{yy}) + \alpha u_x + \beta u_y \qquad\qquad 13$$

An explicit finite difference representation of the equation (13) can be obtained by a forward time center space differencing

$$\frac{u_{i,j}^{n+1} - u_{i,j}^{n}}{\Delta t} = k\left(\frac{u_{i+1,j}^{n} - 2u_{i,j}^{n} + u_{i-1,j}^{n}}{\Delta x^2} + \frac{u_{i,j+1}^{n} - 2u_{i,j}^{n} + u_{i,j-1}^{n}}{\Delta y^2}\right) + \alpha\left(\frac{u_{i+1,j}^{n} - u_{i-1,j}^{n}}{2\Delta x}\right) + \beta\left(\frac{u_{i,j+1}^{n} - u_{i,j-1}^{n}}{2\Delta y}\right) \quad 14$$

By Von Neumann's method

$$E_{p,o,q} = e^{i\vartheta(ph)} . e^{i\gamma(os)} . \varepsilon^q \qquad\qquad 15$$

where $E_{p,o,q}$ is error

$$u(x, y, t_n) = e^{i(\vartheta,\gamma)\binom{x}{y}} = e^{i\vartheta x} . e^{i\gamma y} \qquad\qquad 16$$

Let *x=ph* ,*y=os*. Now substitute in the equation (14):

$$e^{i\vartheta(ph)} . e^{i\gamma(os)} . \varepsilon^{q+1} - e^{i\vartheta(ph)} . e^{i\gamma(os)} . \varepsilon^q =$$

$$K\left(\frac{e^{i\vartheta(p+1)h} . e^{i\gamma(os)} . \varepsilon^q - 2e^{i\vartheta(ph)} . e^{i\gamma(os)} . \varepsilon^q + e^{i\vartheta(p-1)h} . e^{i\gamma(os)} . \varepsilon^q}{\Delta x^2}\right) +$$

$$\frac{e^{i\vartheta(ph)} . e^{i\gamma(o+1)s} . \varepsilon^q - 2e^{i\vartheta(ph)} . e^{i\gamma(os)} . \varepsilon^q + e^{i\vartheta(ph)} . e^{i\gamma(o-1)s} . \varepsilon^q}{\Delta y^2}) +$$

$$\alpha\left(\frac{e^{i\vartheta(p+1)h} . e^{i\gamma(os)} . \varepsilon^q - e^{i\vartheta(p-1)h} . e^{i\gamma(os)} . \varepsilon^q}{2\Delta x}\right) + \beta\left(\frac{e^{i\vartheta(ph)} . e^{i\gamma(o+1)s} . \varepsilon^q - e^{i\vartheta(ph)} . e^{i\gamma(o-1)s} . \varepsilon^q}{2\Delta y}\right) \; 17$$

Divide equation 17 by $(e^{i\vartheta(ph)} . e^{i\gamma(os)} . \varepsilon^q)$ leads to the equation 18:

$$\frac{\varepsilon - 1}{\Delta t} = K\left(\frac{e^{i\vartheta h} - 2 + e^{-i\vartheta h}}{\Delta x^2} + \frac{e^{i\gamma s} - 2 + e^{-i\gamma s}}{\Delta y^2}\right) + \alpha\left(\frac{e^{i\vartheta h} - e^{-i\vartheta h}}{2\Delta x}\right) + \beta\left(\frac{e^{i\gamma s} - e^{-i\gamma s}}{2\Delta y}\right) \qquad 18$$

In a simpler form, we consider $\alpha = \beta$

$$\varepsilon - 1 = \frac{\Delta t K}{\Delta x^2}(2cos\vartheta h - 2) + \frac{\Delta t k}{\Delta y^2}(2cos\gamma s - 2) + \alpha\frac{\Delta t}{\Delta x} isin\, \vartheta h + \alpha\frac{\Delta t}{\Delta y} isin\, \gamma s, \qquad 19$$

Where $r_x = \frac{\Delta t K}{\Delta x^2}$, $r_y = \frac{\Delta t K}{\Delta y^2}$, $\Delta x = \Delta y = 1$ then $r_x = r_y = r$

and   let $\mu_y = \alpha \frac{\Delta t}{\Delta y} \leq 1$ is Courant Fried Richs Lewy (CFL) condition[16]. Where

μ_y *is called CFL* number. In general the explicit finite difference methods will require that

the CFL be bonded by a constant which will depend upon the particular numerical scheme $\mu = \mu_x = \mu_y$ Now substitute in the equation(19):

$$\varepsilon - 1 = 2r(\cos \vartheta h - 1) + 2r(\cos \gamma s - 1) + \mu i \sin \gamma s + \mu i \sin \vartheta h \qquad 20$$

This gives a complex amplification factor, the modulus of which reads

$$\varepsilon \bar{\varepsilon} = |\varepsilon|^2 = \left(1 - 4r\left(\sin^2 \frac{\vartheta h}{2} + \sin^2 \frac{\gamma s}{2}\right)\right)^2 - \mu^2 \left(\frac{\sin \gamma s}{2} + \frac{\sin \vartheta h}{2}\right)^2 \qquad 21$$

Hence $r \leq 1/4$, $\mu \leq 1$ [16]. by Van Neumann stablity condition $|\varepsilon|^2 \leq 1$:

$$(1 - 4r\left(\sin^2 \frac{\vartheta h}{2} + \sin^2 \frac{\gamma s}{2}\right))^2 - \mu^2(\sin \frac{\gamma s}{2} + \sin \frac{\vartheta h}{2})^2 \leq 1 \qquad 22$$

Either

$$(1 - 4r\left(\sin^2 \frac{\vartheta h}{2} + \sin^2 \frac{\gamma s}{2}\right)) - \mu(\sin \frac{\gamma s}{2} + \sin \frac{\vartheta h}{2}) \leq 1 \qquad 23$$

$$-\mu \leq \frac{4r(\sin^2 \frac{\vartheta h}{2} + \sin^2 \frac{\gamma s}{2})}{\sin \frac{\gamma s}{2} + \sin \frac{\vartheta h}{2}} \qquad 24$$

$$\frac{4r\left(\sin^2 \frac{\vartheta h}{2} + \sin^2 \frac{\gamma s}{2}\right)}{\frac{\sin \gamma s}{2} + \frac{\sin \vartheta h}{2}} \approx 1 \qquad 25$$

That lead to $\mu > -1,$ 26

or when : $(1 - 4r\left(\sin^2 \frac{\vartheta h}{2} + \sin^2 \frac{\gamma s}{2}\right)) + \mu(\sin \frac{\gamma s}{2} + \sin \frac{\vartheta h}{2}) \leq 1$ \qquad 27

$$\mu \leq \frac{4r(\sin^2 \frac{\vartheta h}{2} + \sin^2 \frac{\gamma s}{2})}{\sin \frac{\gamma s}{2} + \sin \frac{\vartheta h}{2}} \qquad 28$$

That lead to $\qquad\qquad \mu \leq 1$ $\qquad\qquad\qquad\qquad$ 29

From the equations (26) and (29) get :

$$-1 < \mu \leq 1 \qquad\qquad\qquad 30$$

By CFL condition has the following properties If $\mu = \alpha \frac{\Delta t}{\Delta y} \leq 1$ in 1- dim.Then

$\mu = \mu_y + \mu_x \leq 1$ in 2-dim.

i.e $\qquad\qquad\qquad \alpha_x \frac{\Delta t}{\Delta x} + \alpha_y \frac{\Delta t}{\Delta y} \leq 1 \qquad\qquad 31$

suppose that $\alpha = \alpha_x = \alpha_y$ and $\Delta x = \Delta y$ .Then the equation (31) is become as :

$$2\alpha \frac{\Delta t}{\Delta x} \leq 1 \qquad\qquad\qquad 32$$

And that leads to $2\mu \leq 1$ and $\mu \leq \frac{1}{2}$ when $|\alpha| > 0$.

4. Experimental Results

A different set of 20 natural images selected from the Berkeley Segmentation Dataset and Benchmarks 300 (BSDS300) were used to evaluate the proposed modification of the isotropic model [17]. The suggested method's outcomes are compared with those attained by the original isotropic method. The missing areas in the selected images range in size, allowing us to evaluate how well the suggested improved model restores the missing areas. Virtual masks are used to create gaps in the image in order to test the capability and efficacy of the recommended model by filling them. There are four main types of masks: square, narrow rectangle, big rectangular, and they may be used anywhere in the image. The Matlab programming was used to test the proposed model on the selected standard natural images. Figure 2 shows a group of images selected to test the effect of α and β values on the inpainted images. When $\alpha = \beta = 1/2$,the twigs have been restored perfectly in image in the first and second cases while when α≠ β, the twigs were not good restored with unclear edges. Furthermore, in the third case, the best results were obtained when the value α=0 and β=1where the beach boundaries were restored in the image. Finally, the best inpainted image when α=0 and β=1 compared to other α and β values in the fourth case

	Original images	**Masked images**	**α= 1/2** **β= 1/2**	**α= 1** **β= 0**	**α= 0** **β= 1**
Case1					
Case2					
Case3					
Case4					

Figure2: Effect of α and β values onto the inpainted images using different types of mask.

4.1 Image Quality Assessment

The effectiveness of the suggested model will be evaluated together with the quality of the inpainted images using three separate statistical quality measures. These quality indicators can be used to compare the original and painted images' quality. First, the mean square error (MSE) will be used to determine the difference between the original image *I* provided by [8] and the inpainted image *I'*.

$$MSE = \frac{1}{(NMR)}\sum_{q=1}^{Q}\sum_{n=1}^{N}\sum_{m=1}^{M}[\,I_q(n,m) - I'_q(\,n,m)\,]^2 \quad , \qquad 33$$

where q is the number of channels in a color image, n is the number of rows and m is the number of columns in the channel. Secondly, the other measure is the peak signal to noise ratio (PSNR) which can be found in [8]:

$$PSNR = 10\log_{10}(\frac{255^2}{MSE}) \qquad\qquad 34$$

Best quality of the inpainted image gets when the value of PSNR is high and MSE is low. Finally, the Structural Similarity Index (SSIM) is used to measure the similarity between original and inpainted images. The SSIM can be estimated using the relationship [8]:

$$SSIM(I,I') = \frac{(2\mu_I\mu_{I'}+c_1)(2\sigma_{II'}+c_2)}{(\mu_I^2+\mu_{I'}^2+c_1)(\sigma_I^2+\sigma{I'}^2+c_2)} \quad , \qquad\qquad 35$$

where (μ_I, σ_I) and $(\mu_{I'}, \sigma_{I'})$ refers to mean and standard deviation of patches in the images I and I', respectively; $\sigma_{II'}$: the covariance of I and I'; $c_1 = (k_1 h)^2$, $c_2 = (k_2 h)^2$ such that h = $2^{bits\ per\ pixel} - 1$, $k_1 = 0.01$ and $k_2 = 0.03$. However, the value of SSIM is range from 1 to 0 and when the value is 1 means the two images are identical while 0 values refer to not identical. Thus, the qualities of inpainted images increase when the value of SSIM increases to be near 1.

To test the proposed model compared with the classic model, four types of masks are selected with different images. The proposed model is used with α=1 and β=0 to recover the square missing region in case 1, the inpainted image had better restoration to the missing region with clearer edges compared with the inpainted image obtained using the isotropic model as shown in Figure 3. In case 2, the selected missing region is chosen as a narrow horizontal rectangular line as shown in Figure 4b. Furthermore, restoration of the missing region and edges using a modified isotropic model with α=1 and β=0 enhances the treated images where the edges appeared clearer with less blurry compared with the classic model as shown in Fig. 4.

Figure3: Case1 of image inpainting (a) original image, (b) masked image, (c) and (d) inpainted image using isotropic model and proposed model, respectively.

Figure 4: Case2 of image inpainting (a) original image, (b) masked image, (c) and (d) inpainted image using isotropic model and proposed model, respectively.

In case 3, a narrow vertical rectangular missing area is selected (Figure 5b). Using the proposed model with α=0 and β=1 significantly reduced blurring and enhanced the recovery of the missing area as well as edges compared with the inpainted image obtained using the classic model as shown in Figure 5. Finally, Case 4 represents a large rectangular missing area extending horizontally on the image (Figure 6b). When using the modified isotropic model with α=1 and β=0, the blurring significantly decreased and the edges appeared partially in the painted area compared with the inpainted image obtained using the classic model as shown in Fig. 6.
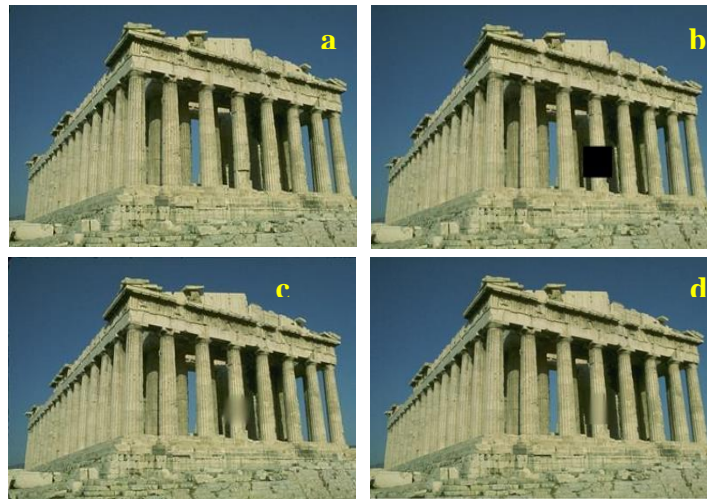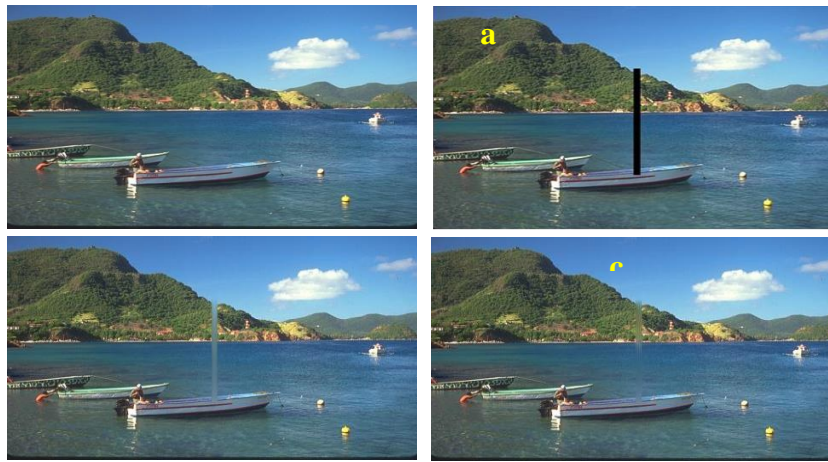
Figure 5: Case3 of image inpainting (a) original image, (b) masked image, (c) and (d) inpainted image using isotropic model and proposed model, respectively.

Figure 6: Case4 of image inpainting (a) original image, (b) masked image, (c) and (d) inpainted image using isotropic model and proposed model, respectively.

The MSE, PSNR, and SSIM values of these cases with different α and β values are introduced in Tables 1, 2, and 3, respectively. These tables prove the proposed model is able to fill rregion effectively and gives higher PSNR values with low MSE values and the SSIM values are close to 1. The proposed technique obtained higher values of SSIM and PSNR with low MSE values than the classical model as seen in Tables 1, 2, and 3, that mean the inpainted regions obtained by the proposed model are more coherent with the rest of the images for all these cases when $\alpha = 0$ and $\beta = 1$.

Table 1: MSE values or four shapes of missing region

α	β	Case1	Case2	Case3	Case4
1/2	1/2	33.3438	35.0851	29.6715	29.8571
1	0	33.4896	34.5266	30.3180	29.6170
0	1	32.6728	36.8375	31.2121	31.1774

Table 2: PSNR values for four shapes of missing region

α	β	Case1	Case2	Case3	Case4
1/2	1/2	53.287	37.922	78.462	82.636
1	0	54.691	41.318	83.914	84.261
0	1	57.180	29.361	56.330	76.184

Table 3: SSIM values for four shapes of missing region

α	β	Case1	Case2	Case3	Case4
1/2	1/2	0.477	0.657	0.334	0.393
1	0	0.458	0.636	0.328	0.410
0	1	0.484	0.641	0.475	0.362

The values of MSE, PSNR, and SSIM from images that were inpainted using the classic isotropic model and the suggested model with various values of α and β are listed in Table. The image quality confirmed that the proposed model is outperforming the classical model. The suggested model is efficient, able to fill in the empty space, and provides higher PSNR values with minimal MSE. The data showed that, when the suggested model was put up against the original model, the

SSIM value increased, indicating that the inpainted models seem to be closer to the originals. Additionally, there has been a very noticeable improvement over time.

Table 4: Image inpainted quality assessment comparison using MSE, PSNR, and SSIM.

Cases	Model	MSE	PSNR	SSIM	Time (S)
Case1	Isotropic	22.85881	34.68158	0.63376	39.8294
	Modified isotropic	11.43862	38.21239	0.60564	1.88148
Case2	Isotropic	23.88252	34.38542	0.88483	2.77682
	Modified isotropic	12.20463	37.30076	0.93475	0.68811
Case3	Isotropic	30.92779	33.48105	0.78239	111.222
	Modified isotropic	22.01346	35.07477	0.80704	13.9987
Case4	Isotropic	72.54162	30.23256	0.47157	389.569
	Modified isotropic	47.29332	34.22688	0.46518	8.9966

5. Conclusions

The modified isotropic model gives good results if the missing areas are small, but the efficiency of the equation in repainting is less. If the areas are large in applying the isotropic equation, all the results are blurry, while the use of the modified isotropic model, can partially recover the edges and more clarity, the model succeeds when the direction of the stretching of the texture outside the region in the direction of the spread of additive derivative and the result improves as the surrounding area of missing area is less textured. In the future, different operators can be used to modify the isotropic diffusion model. To develop an inpainting application, it is best to use an automatic technique to recover large missing areas. The gradient magnitude can be used to study

the geometrical direction of surrounding areas that help to select the better direction for recovering the missing regions. Also, this work can be enhanced by using other kinds of PDE methods.

References

[1] Z Qin, Q Zeng, Y Zong, F Xu, Image inpainting based on deep learning: A review, Displays 69 (2021) 102028, https://doi.org/10.1016/j.displa.2021.102028

[2] F Berntsson, G Baravdish, Coefficient identification in PDEs applied to image inpainting, Applied Mathematics and Computation, 242(2014)227-235, https://doi.org/10.1016/j.amc.2014.05.051

[3] A Theljani, Z Belhachmi, M Moakher, High-order anisotropic diffusion operators in spaces of variable exponents and application to image inpainting and restoration problems, Nonlinear Analysis: Real World Applications, 47(2019) 251-271, https://doi.org/10.1016/j.nonrwa.2018.10.013.

[4] X Zhu, Y Qian, X Zhao, B Sun, Y Sun, A deep learning approach to patch-based image inpainting forensics, Signal Processing: Image Communication, 67(2018)90-99, https://doi.org/10.1016/j.image.2018.05.015

[5] T Xu, T Z Huang, L J Deng, X L Zhao, J F Hu, Exemplar-based image inpainting using adaptive two-stage structure-tensor based priority function and nonlocal filtering, Journal of Visual Communication and Image Representation, 83(2022)103430, https://doi.org/10.1016/j.jvcir.2021.103430

[6] S. Masnou, J.-M. Morel, Level lines based disocclusion, in Proceedings 1998 International Conference on Image Processing. ICIP98, 3(1998)259–263, http://dx.doi.org/10.1109/ICIP.1998.999016.

[7] M. Bertalmio, G. Sapiro, V. Caselles, C. Ballester, Image inpainting, in In Proc. ACM Conf. Comput. Graph., (2000) 417–424.

[8] A Halim, B.V. Rathish Kumar, An anisotropic PDE model for image inpainting, Computers and Mathematics with Applications, 79(2020)2701-2721, https://doi.org/10.1016/j.camwa.2019.12.002

[9] A Theljani, Z Belhachmi, M Moakher, High-order anisotropic diffusion operators in spaces of variable exponents and application to image inpainting and restoration problems, Nonlinear Analysis: Real World Applications, 47(2019)251-271, https://doi.org/10.1016/j.nonrwa.2018.10.013

[10] A. K. Al-Jaberi, A Asaad, S.A. Jassim, N. Al-Jawad ,Topological data analysis to improve exemplar-based inpainting", Proc. SPIE 10668, Mobile Multimedia/Image Processing, Security, and Applications 2018, 1066805, https://doi.org/10.1117/12.2309931

[11] Z Wang, A.C Bovik, H R. Sheikh, and Eero P. Simoncelli, "Image Quality Assessment: From Error Visibility to Structural Similarity" IEEE Transactions on Image Processing, 13(2004)

[12] K R. Patel, L Jain, A G. Patel, Image inpainting, a review of the underlying different algorithms and comparative study of the inpainting techniques, International Journal of Computer Applications 118(2015)32-38.

[13] Gi Aubert, P Kornprobst, Mathematical Problems in Image processing Partial Differential Equations and the Calculus of Variations, 2nd edition, Springer, 2006.

[14] C Guillemot, O L Meur, Image Inpainting: Overview and Recent Advances, IEEE Signal Processing Magazine, 31(2014)127-144, DOI: 10.1109/MSP.2013.2273004

[15] A k Aljaberi, E M. Hameed, A review of PDE-based local inpainting methods, J Phys. Conference Series 1818 (2021) 012149, doi:10.1088/1742-6596/1818/1/012149

[16] M.N. Özisik¸ H.R.B. Orlande, M.J. Colaço, R.M. Cotta, Finite Difference Methods in Heat Transfer, 2ed, Taylor & Francis Group, LLC, USA, 2017.

[17] P Arbelaez, C.F, D.M., 2007. The Berkeley Segmentation Dataset and Benchmark. The website of the Berkeley database is. Available at: https://www2.eecs.berkeley.edu/Research/Projects/CS/vision/bsds/

تقنية جديدة للطلاء الداخلي للصور تعتمد على انتشار الخواص

زينب علي عبد الكريم[1] و احمد كاظم الجابري[2]

1 قسم الرياضيات ، كلية العلوم ، جامعة البصرة ، البصرة ، العراق

2 قسم الرياضيات ، كلية التربية للعلوم الصرفة ، جامعة البصرة ، البصرة ، العراق.

المستخلص

تم اقتراح تقنية جديدة معتمدة على نموذج الانتشار isotropic model لاستعادة المناطق المفقودة في الصورة الرقمية تعتمد هذه التقنية على تعديل نموذج الانتشار الكلاسيكي classical isotropic model. وتم تطبيقه على الصور الطبيعية لاستعادة المناطق المفقودة المختلفة في الشكل والمساحة وتمت مقارنة نتائج النموذج المعدل مع النموذج الكلاسيكي التي تم الحصول عليها وتبين تفوق النموذج المعدل على النموذج الكلاسيكي من حيث بناء النسيج في المنطقة المفقودة واستعادة المناطق الكبيرة تم استخدام العديد من مقاييس الجودة لحساب فعالية النموذج المقترح مثل MSEو PSNR وSSIM يظهر النموذج المعدل معايير جودة افضل لعدد كبير من الصور الطبيعية مع أداء افضل مقارنة بنموذج الانتشار الكلاسيكي